FOREX Publication
Open Access | Rapid and quality publishing

International Journal of
Electrical and Electronics Research (IJEER)
Research Article | Volume 11, Issue 4 | Pages 1167-1175 | e-ISSN: 2347-470X

Design of Boost Integrated Luo Converter for Grid Tied EV Based Charging Station

Vimalraj Ambeth Vijayarangan[1] and Saravanan Kaliyaperumal[2]

[1]Research Scholar, Department of Electrical and Electronics Engineering, SRM Institute of Science and Technology, Kattankulathur, Chennai, India; vijayambeth@gmail.com
[2]Associate Professor, Department of Electrical and Electronics Engineering, SRM Institute of Science and Technology, Kattankulathur, Chennai, India; saravank3@srmist.edu.in

***Correspondence:** Vimalraj Ambeth Vijayarangan; *vijayambeth@gmail.com*

ABSTRACT- The combination of Renewable Energy Source (RES) and storage element in charging station is a possible solution for meeting the growing energy requirement of electric vehicles (EVs). In a grid-tied RE system, the converters are essential for attaining the process of power conditioning. Conventional DC-DC converters suffer from issues like voltage spikes, electromagnetic interference, and efficiency losses. The necessity for integrated converters arises from the demand for improved power conditioning, increased power density, and enhanced overall system performance. As a result, in this work, boost integrated Luo converter is proposed due to the ability to address aforesaid drawbacks and offer superior power conditioning capabilities in modern power electronic systems. The Luo converter with conventional boost converter aids in alleviating the current ripples to a greater extent. The PI control with Particle Swarm Optimization (PSO) strategy is efficiently employed in this study as provides consistent voltage supply to the converter. Thus, the ultimate aim of this work is achieved by enhancing the low dc voltage of PV panel by using a PSO-PI control-based hybrid converter, which increases its efficiency, lowers the cost, supplies suitable current and voltage for energizing the battery or to charge the grid tied EV charging station. The simulation results obtained verifies the effectiveness of developed system.

Keywords: RES, EV, PV panel, DC-DC converters, Boost integrated Luo Converter, PSO-PI control.

ARTICLE INFORMATION

Author(s): Vimalraj Ambeth Vijayarangan and Saravanan Kaliyaperumal;
Received: 28/06/2023; **Accepted**: 11/09/2023; **Published**: 23/12/2023;
e-ISSN: 2347-470X;
Paper Id: IJEER230728;
Citation: 10.37391/IJEER.110438
Webpage-link:
https://ijeer.forexjournal.co.in/archive/volume-11/ijeer-110438.html

1. INTRODUCTION

The impact of increased mobility and better living standard results in higher energy consumption, which causes emission of greenhouse gasses and tremendous pollutions of environment [1]. In order to avoid the emission of greenhouse gases and to improve the transportation industry's economic or environmental challenges, the Electric vehicles (EVs) have been occurred as a best possible solution. Therefore, the electrified transportation networks are essential for lowering the fossil fuel usage and carbon emissions. Through the progress of EV sector and the improvement of batteries, the EV has become a valuable element as it is capable of transmitting the electricity in both directions [2-4]. On the other hand, the transportation industries are shifting from thermal to renewable energy resources due to global warming and depletion of fossil fuels [5]. In general, charging an EV requires a substantial quantity of electrical energy, which is usually supplied by coal or gas fired power plants. This actually leads to fossil fuel depletion and global warming. To make the EVs completely clean and green, the required electrical energy for running the EV is derived from the RE sources like PV, wind and so on.

When the EVs are grouped in a charging station, large amount of electricity is consumed, which has a significant influence on the grid operation. As a result, integrating a RE system with an energy storage battery is viewed as the best approach for tackling this issue [6, 7]. Solar energy, in this opinion, is the most potential energy source for substituting fossil fuels such as natural gas, coal, and petroleum products. It is possible to integrate PV cells into roofs of battery powered EVs [8, 9]. Recent reductions in battery system costs, combined with its excellent support capabilities, have made the integration of PV with battery systems economically feasible. [10-12]. In the proposed system, batteries [13] are used to store excess energy generated by the solar panels during periods of high solar production. These batteries act as a buffer, allowing the system to supply electricity to the grid during low solar output or at night when solar panels are not producing power. This energy storage [14, 15] capability enhances grid stability, provides backup power, and optimizes energy utilization, ultimately increasing an overall reliability and efficiency of the grid tied system.

For the purpose of producing constant voltage output and optimizing the low dc voltage, which is produced by the PV, a DC-DC converter is implemented [16, 17]. The DC-DC step up converters is designed to convert the low dc voltage levels to

FOREX Publication
Open Access | Rapid and quality publishing
International Journal of Electrical and Electronics Research (IJEER)
Research Article | Volume 11, Issue 4 | Pages 1167-1175 | e-ISSN: 2347-470X

higher voltage levels by retaining the input voltage [18]. This is because the input voltage level is crucial in determining efficiency and performance of converter. By maintaining input voltage levels, the converter operates in a favorable range, reducing voltage stress on components and minimizing losses. To get maximum voltage gain, a traditional boost converter is used, which has high voltage boosting efficiency but it requires high duty ratio. The buck boost converter is chosen to step up the low DC voltage, but its parasitic resistance restricts maximum voltage gain, and larger duty ratios impact performance. Additionally, high input current ripples and distorted output voltage reduce converter efficiency [19]-[21]. The preceding converters' restrictions are overcome by using a Cuk converter, which employs a soft switching mechanism to decrease the circuit's control complexity. Nevertheless, this converter has a significant disadvantage in that it contains a high number of reactive components, resulting in high current stress throughout the device. Although SEPIC converters have a stable input current, the excessive current ripples hinder the maximum power extracting performance of the PV [22, 23]. The article describes all of these modes in detail, as well as the architecture of the components. The outcomes of both theoretical and experiments for a 1-kW setup based on the proposed configurations are presented. On the other hand, Luo converters are regarded as highly efficient in terms of power conversion [24]. It has low duty cycle and high voltage conversion efficiency. Moreover, this converter topology is designed to produce a large output gain while maintaining a constant voltage lifting capability by resolving all of the previous concerns [25]. To address these problems, an efficient high gain boost integrated Luo converter is thus proposed in this work, which boosts voltage gain while reducing the ripples.

The control method used in this work ensures a consistent voltage supply to the converter. Employing PI control proves to be an effective and straightforward approach that delivers favorable outcomes. [26, 27]. Moreover, PI controller improves its viability and efficiency of the converter [28]. When the comparator compares actual voltage signal to the reference voltage signal, it generates an error signal, which is sent to PI controller. It performs voltage regulation and then send regulated voltage to PWM generator, which generates suitable PWM signals for a power converter. The utilization of optimization strategy improves the efficiency of PI controller by accelerating the rising time and eliminating steady state inaccuracy [29, 30]. Ziegler-Nichol's method offers a simple and quick approach for PI controller tuning, but it is not be suitable for all types of systems, particularly those with complex dynamics or specific performance requirements. More advanced tuning which involves Genetic Algorithms, a population-based optimization technique inspired by process of natural selection, where potential solutions evolve over generations. However, the probabilistic nature makes the optimization process complex and results in slow convergence. As a result, the proposed work introduces PSO approach which optimize the controller's performance and ensure stability and accuracy in the control system. [31].
Boost integrated Luo converter is used here to optimize the PV panel's output voltage. To regulate generated output of the converter and to improve its efficiency, a PSO-PI controller is utilized, which avoids the PI parameter tuning complexity in a wider range. Additionally, battery is incorporated to meet power demand during peak hours. The enhanced output voltage, which is generated by the proposed converter, is injected into grid through a 1ϕ VSI. Before injecting the voltage into the grid, it is filtered by using LC filter, which removes the noise and distortion in the signal. With an assistance of a conventional PI controller, the operational efficiency of the VSI is also regulated.

2. PROPOSED SYSTEM METHODOLOGY

The process of charging an electric vehicle requires a significant quantity of electrical energy, which is sufficiently provided by the renewable PV system. In the current scenario, the integration of PV and battery has become economically feasible because of possessing multiple beneficial factors like minimum cost of battery systems and the maximum supporting capability. When the EVs are clustered in a charging station, a large amount of electricity is consumed, which has a significant impact on the grid operation. Thus, the integration of RE generation with battery is viewed as the optimum solution for meeting the energy demand without any interruption.

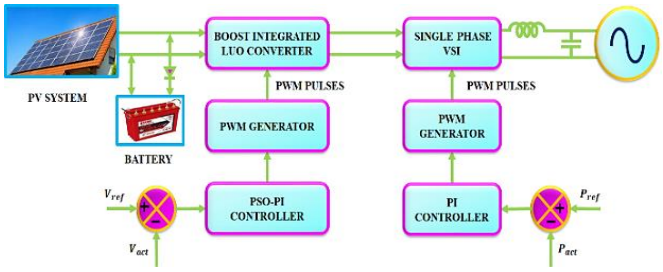

Figure 1: Circuit representation of PV module

The PV generates low DC voltage, which is not sufficient for operating the grid tied EV charging station and so the generated low DC voltage of PV is enhanced by implementing the boost integrated Luo Converter. The proposed converter combines the operation of both boost and Luo converter to provide a high output gain and low duty cycle. Since output of the PV is not stable, an improved output voltage of the converter is unsteady, which is thus regulated through the implementation of PSO tuned PI control approach. The comparison of V_{act} with V_{ref} is carried out and an error is then fed as the input of PSO-PI controller, which constantly regulates the converter output with the assistance of a PWM generator. Furthermore, batteries are incorporated in PV-fed EV stations with grid to store excess solar energy during periods of high PV generation. This stored energy is utilized during low solar output or at night to charge EVs and provide continuous power supply to EV charging station. The battery integration improves grid stability, enhances the station's energy resilience, and reduces dependency on the grid during peak demand periods. The regulated DC link voltage is then given to a 1ϕ VSI for performing DC to AC conversion in an enhanced manner. The operational efficiency of the VSI is maximized with the help of the traditional PI controller and so the charge, which is delivered to the grid-connected EV based charging station is

FOREX Publication
Open Access | Rapid and quality publishing
International Journal of Electrical and Electronics Research (IJEER)
Research Article | Volume 11, Issue 4 | Pages 1167-1175 | e-ISSN: 2347-470X

phenomenally regulated. The inverter output is then filtered by using the LC filter before injecting it into the grid, which assists in eliminating the noise and distortion in the grid signal. The contribution of proposed work involves.

- Development of Boost integrated Luo converter for enhancing PV voltage, and for mitigation of current ripples.
- PSO-PI controller to ensure consistent voltage supply to converter.
- Adoption of battery to achieve uninterruptable grid supply.

Overall, this work contributes to the advancement of power electronic systems by proposing and implementing a novel hybrid DC-DC converter with enhanced power conditioning capabilities for PV applications.

3. MODELLING OF PROPOSED SYSTEM

3.1 PV System

As the eminence of PV system is significantly maximum in the process of power generation, it is given prior importance in this section to validate present study with the necessary elements and so the single diode archetype of PV is clearly represented in *figure 2*. It includes the portrayal of the electrical parameters like arrays, modules, panels and PV cells for signifying the physical features of PV system. The figure indicates that the diode *D*, resistance R_{sh} and the current source I_{ph} are linked in a parallel manner. In addition, the load is linked in series with the resistance R_{se} for generating the load branch whereas this branch of load is parallelly linked to with the source end legs of PV. Hence, the PV modeling is elaborately portrayed with significant illustration of the components.

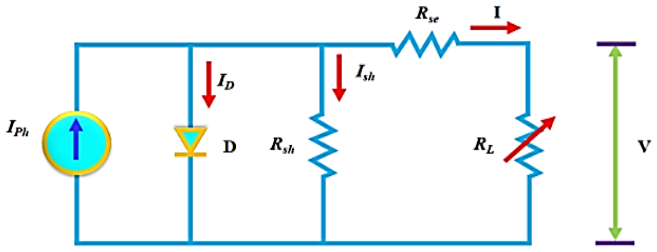

Figure 2: Single diode model of PV

The modeling or design of the PV is illustrated through the subsequent experiential equation. It begins with the photo current design, which is represented as,

$$I_{ph} = [I_{SC} + K_i(T - 298)] * \frac{\lambda}{1000} \quad (1)$$

Here, the insolation is indicated as λ, operating temperature of the module is indicated as T, PV's short circuit current is signified as I_{SC} and the current temperature coefficient is signified as K_i. The dependence of this photo current model is significantly high on both the temperature and insolation.
To evaluate I_{rs} (modules' saturation current), the subsequent equation is used as,

$$I_{rs} = \frac{I_{SC}}{e^{\left(\frac{qV_{OC}}{N_S KAT}\right)} - 1} \quad (2)$$

Here, I_{SC} specifies short circuit current, K specifies the Boltzmann constant (1.3805×10^{-23}J/K), N_s signifies series linked cells' number, q signifies the charge of electron, I signifies the Ideal factor and V_{OC} signifies an open circuit voltage of PV.

The of the module saturation current (I_o) is mentioned as,

$$I_o = I_{rs}\left[\frac{T}{T_r}\right]^3 e^{\left[\frac{q*Ego}{BK}\left(\frac{1}{T_r} - \frac{1}{T}\right)\right]} \quad (3)$$

Here, the silicon band gap (1.1eV) is indicated as E_{go}, the ideality factor is indicated as A and the reference temperature 0 The current of PV module (IPV) is represented as,

$$I_{PV} = N_p * I_{ph} - N_p * I_o\left[e^{\left[\frac{q*(V_{PV} + I_{PV}R_{se})}{N_S AKT}\right]} - 1\right] \quad (4)$$

Here, the yield voltage of PV is specified as V_{PV} whereas the parallel linked panels' quantity is specified as N_p.

The PV output is then fed as an input of the proposed converter, which aids in the process of enhancing the low voltage of PV in a wider range.

3.2 Boost Integrated Luo Converter

The hybrid topology of integrating the boost and Luo converters is implemented in this study to maximize the ratio of voltage gain and to attain the constant regulation of output voltage in a wider range. Because it is highly capable of maintaining consistent input and output currents, this converter's function makes a significant contribution to the total system performance. The circuit diagram of this converter is phenomenally portrayed in *figure 3*. The boost integrated Luo converter is also utilized as a voltage multiplier circuit. It achieves this by selectively switching between multiple input voltage sources to provide an output voltage. The converter operates in a continuous conduction mode (CCM) and incorporates a coupled inductor, which enables high voltage gain and efficient power conversion. The capacitor and inductor at output side of converter acts LC Filter resulting in more stable continuous output with reduced voltage ripple and leads to better power transfer and utilization.

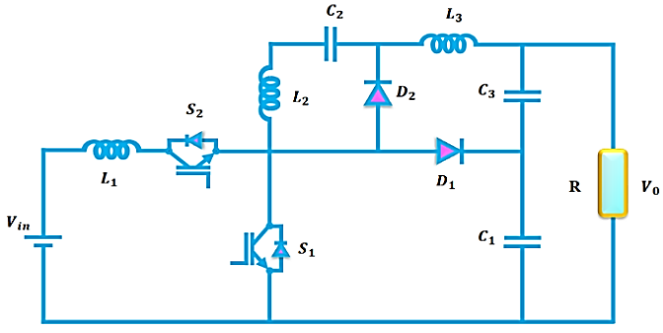

Figure 3: Circuit diagram of proposed converter

FOREX Publication
Open Access | Rapid and quality publishing
International Journal of Electrical and Electronics Research (IJEER)
Research Article | Volume 11, Issue 4 | Pages 1167-1175 | e-ISSN: 2347-470X

This circuit includes Inductors ($L_1, L_2, L_3,$) diodes (D_1, D_2), switches (S_1, S_2), and capacitors ($C_1, C_2, C_3,$), which are significantly linked with the input voltage (V_{in}) for enhancing the voltage in a wider range. Moreover, the output voltage gets possibly changed by varying the switch ON time since the converter's output voltage has high dependence over the control switch and duty cycle. Hence, the subsequent equation is used for computing the output voltage for duty cycle D, which is expressed as,

$$\frac{V_0}{V_{in}} = \frac{1}{(1-D)} \quad (5)$$

Here, the duty cycle is specified as D whereas an output and input voltages are specified as V_0 and V_{in}. Furthermore, both the output and input powers are proportional to each other in the ideal circuit, which is expressed as, t_1 to Ts. Switch S is turned off throughout the interval. Cascaded energy from the reactive elements L_1 , L_2 and C_2 , as well as the input source V_S, is transmitted to the load side. The cascaded discharge of energy into the load side produces a massive rise in dc-voltage gain at output. In this case, inductor L_1 supplies current to the inductor L_2 while simultaneously charging the capacitor C_1.

$$P_0 = P_{in} \Rightarrow V_0 I_0 = V_{in} I_{in} \quad (6)$$

In this study, the boost converter's inductor and capacitor values are computed through the subsequent *equations (7)* and *(8)* as,

$$L_1 = \frac{V_{in}}{f_s \Delta I_{L1}} D \quad (7)$$

Here, the ripple in input current is indicated as ΔI_{L1} whereas the switching frequency is indicated as f_s.

$$C_1 = \frac{I_{out}}{f_s \Delta V_0} D \quad (8)$$

Here, the ripple in output voltage is specified as ΔV_0.

The Inductors' values of Luo converter are specified as follows,

$$L_2 = \frac{DTV_{in}}{\nabla IL_2} \quad (9)$$

$$L_3 = \frac{DTV_{in}}{\nabla IL_3} \quad (10)$$

Here, ∇IL_2 and ∇IL_3 represent the peak-to-peak current values of Inductors L_2 and L_3. In addition, T specifies the Time D specifies Duty cycle. The subsequent equations are utilized to compute values ∇IL_2 and ∇IL_3 as,

$$\nabla IL_2 = \frac{DTV_{in}}{L_2} \quad (11)$$

$$\nabla IL_3 = \frac{DTV_{in}}{L_3} \quad (12)$$

The voltage across C_2 is computed as,

$$VC_2 = \frac{D}{1-D} V_{in} \quad (13)$$

Here, V_{in} specifies an input voltage and D represents duty cycle.

The converter operates in different modes, which are exponentially described in the following section

3.2.1 Mode 1

In this state, the inductor current gets increased and the energy is stored in L_1 during ON condition of S_1 whereas the energy, which is stored in inductor gets delivered to the load during the Switch OFF condition.

The voltage through the inductor gets added with V_{in} for providing the enhanced voltage to the load when the inductor current gets decreased. The converter operation in *mode 1* is remarkably highlighted in *figure 4*.

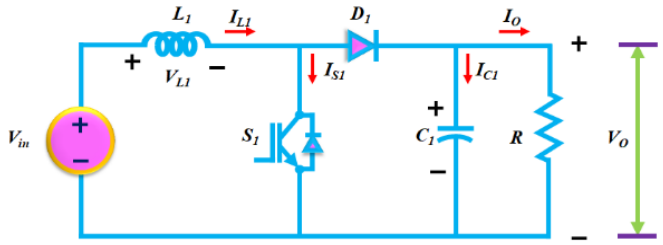

Figure 4: Mode 1 Operation

The state equations for the ON state of S_1 are specified as follows as,

$$\frac{di_{L_1}}{dt} = \frac{V_{L_1}}{L_1} \quad (14)$$

$$\frac{dV_0}{dt} = \frac{V_0}{RC_1} \quad (15)$$

Furthermore, the state equations for the OFF state of S_1 are expressed as follows as,

$$\frac{di_{L_1}}{dt} = \frac{V_{L_1}}{L_1} - \frac{V_0}{L_1} \quad (16)$$

$$\frac{dV_0}{dt} = \frac{i_{L_1}}{C} - \frac{V_0}{C_1 R} \quad (17)$$

As a result, the functioning of the converter in this mode is extremely important in the process of increasing the output voltage.

3.2.2 Mode 2

In this state, the Inductor L_2 gets charged by V_{in} whereas Inductor L_3 gets the energy from C_2 and source during the ON condition of S_2. Meanwhile, C_3 supplies the voltage to load. Similarly, the current, which is drawn from the source, gets turned as zero in the OFF state of S_2.

In order to charge C_2, the current (IL_2) passes through the diode D_2 whereas IL_3 passes through Diode D_2 capacitor C_3 and resistance R for the constant current flow of IL_3. The converter operation in *mode 2* is clearly portrayed in *figure 5*.

FOREX Publication
Open Access | Rapid and quality publishing
International Journal of Electrical and Electronics Research (IJEER)
Research Article | Volume 11, Issue 4 | Pages 1167-1175 | e-ISSN: 2347-470X

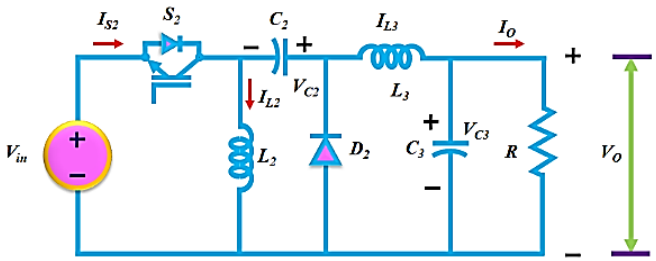

Figure 5: Mode 2 Operation

The capacitor C_2 is charged by IL_3 in the OFF state of S_2 and discharged by IL_2 in the ON state of S_2, which is expressed as,

$$\nabla VC_2 = \frac{1-D}{C_2}\, TI_2 \tag{18}$$

From the aforementioned equation, the value of C_2 is computed as,

$$C_2 = \frac{1-D}{\nabla VC_2}\, TI_2 \tag{19}$$

The output of this converter is controlled by a PWM generators and the PSO aided PI control system.

4. PSO-PI CONTROLLER

As the PSO is capable of generating the optimal outcomes, it is preferably used in the process of tuning the PI variables of K_p and K_i, which is regarded as the prime function of controlling the converter output. In addition, the contribution of this PSO algorithm is significantly high in the process of minimizing both the issues of steady state error and peak overshoot. Moreover, the operating principles of this PSO are highly dependable on the flocks of birds and shoals of fish in accordance with the fitness function and problem constraints.

The process of eliminating the THD and error is magnificently accomplished by determining the objective function of searching area. In general, eight different parameters of decoupled PI controllers like $K_p^v, K_i^v, K_p^Q, K_i^Q, K_p^d, K_i^d, K_p^q, K_i^q$ are categorized as the problem constraints of PV integrated grid system.

The particles in this approach moves in search of the best outcome at each iteration that continues till the best outcome is found, which is greater than the previous one. The velocity of i^{th} particle of swarm in the search space vector is specified as $V_i = [V_{i1}, V_{i2}, \ldots, V_{iD}]$, the position of the search space vector is specified as $X_i = [X_{i1}, X_{i2}, \ldots, X_{iD}]$ and, the i^{th} particle for previous best outcome is specified as $P_i = [P_{i1}, P_{i2}, \ldots, P_{iD}]$ as well as the global best outcome is specified as $P_g = [P_{g1}, P_{g2}, \ldots, P_{gD}]$. The updated location along with velocity of each particle are stated as follows for next iteration,

$$V_i^{n+1} = \omega V_i^n + C_1 r_1 (P_i^n - X_i^n) + C_2 r_2 \left(P_g^n - X_g^n\right) \tag{20}$$

$$X_i^{n+1} = X_i^n + V_i^{n+1} \tag{21}$$

Where $(i = 1,2, \ldots\ldots, m)$, weight of inertia is specified as ω, number of iterations is specified as n, social rate is specified as C_1, cognitive rate is specified as C_2, r_1 and r_2 specifies the random intervals of (0,1).

The following are the steps that compose PSO:

Step 1: Initialize the parameters like $N, LB, UB, I, C_1, C_2, V, w, NV$. From these parameters, population number is specified as N, lower bound is specified as LB, upper bound is specified as UB, maximum iteration number is specified as I, weight coefficients are specified as C_1, C_2, velocity is specified as V, inertia constant is specified as w and variable number is specified as NV.

Step 2: Set the constraints of upper and lower limits. Here, the former is set as $(l_1, l_2, l_3, l_4, l_5, l_6, l_7, l_8)$ whereas the latter is set as $(u_1, u_2, u_3, u_4, u_5, u_6, u_7, u_8)$ for performing the further operations.

Step 3: The variables of PI are defined as $K_p^v, K_i^v, K_p^Q, K_i^Q, K_p^d, K_i^d, K_p^q, K_i^q$. In accordance with the elements like number of both the population N and variable NV, the swarms are initialized as zero.

$$\text{Swarm} = \text{zeros}\begin{bmatrix} X_{1,1} & X_{1,2} & \cdots & X_{1,NV} \\ X_{2,1} & X_{2,2} & \cdots & X_{2,NV} \\ \vdots & \vdots & \ddots & \vdots \\ X_{N,1} & X_{N,2} & \cdots & X_{N,NV} \end{bmatrix} \tag{22}$$

Step 4: The generated swarm populace is equivalent to NV ∗ N matrix, which is specified as,

$$X_{i,j} = \text{round}\left((LB_i + UB_i) * \left(UB_j - LB_j\right)\right) \tag{23}$$

Where $i = 1,2, \ldots, N, j = 1,2, \ldots NV$

In a population vector, the initialization value is signified as,

$$\text{Swarm} = \begin{bmatrix} X_{1,1} & X_{1,2} & \cdots & X_{1,NV} \\ X_{2,1} & X_{2,2} & \cdots & X_{2,NV} \\ \vdots & \vdots & \ddots & \vdots \\ X_{N,1} & X_{N,2} & \cdots & X_{N,NV} \end{bmatrix} \tag{24}$$

Step 5: The generated particle of novel swarm is enhanced and it stores the best experience of P_{best} along with G_{best} in its memory. The swarm's updated velocity is thus mentioned as,

$$V_{i,j}^{i+1} = \omega V_{i,j}^t + C_1 \text{rand}[0,1] X \left(P_{best_{i,j}}^t - X_{i,j}^t\right) + C_2 \text{rand}[0,1] X \left(G_{best_{i,j}}^t - X_{i,j}^t\right) \tag{25}$$

The swarm's updated location is specified as,

$$X_{i,j}^{t+1} = V_{i,j}^{t+1} + X_{i,j}^t \tag{26}$$

Step 6: The fitness function is established; the novel vector is improved in accordance with the rule; the G_{best} along with P_{best} are updated.

FOREX Publication
Open Access | Rapid and quality publishing
International Journal of Electrical and Electronics Research (IJEER)
Research Article | Volume 11, Issue 4 | Pages 1167-1175 | e-ISSN: 2347-470X

If fitness$\left(X_{i,j}^{t+1}\right) <$ fitness $\left(P_{best_{i,j}}^{t}\right)$ then,

$$P_{best_{i,j}}^{t} = X_{i,j}^{t+1} \quad (27)$$

End

If fitness $\left(P_{best_{i,j}}^{t}\right) <$ fitness(G_{best}) then,

$$G_{best} = P_{best_{i,j}}^{t} \quad (28)$$

Step 7: If the iteration number is exceeded to the maximum level, end the program or repeat *steps* 5 & 6 . The Flow representation of PSO-PI controller is remarkably illustrated in *figure 6*.

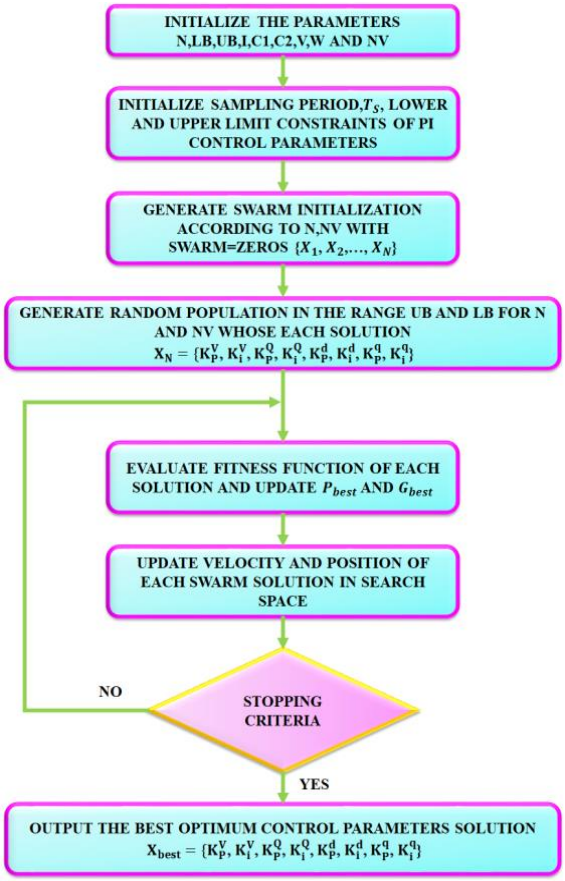

Figure 6: Flow representation of PSO-PI controller

The PSO-PI controller's trial and error process is highly time consuming. Thus, the instigation of this approach provides best optimal K_p and K_i values with fast response.

The regulated converter output is then given as the input of a 1ϕ VSI, which assists in the processes of DC-AC conversion to synchronize the grid voltage in a significant manner. Furthermore, the inverter output is constantly regulated by employing the PI controller and the distortions or noises in the output voltage are eliminated with the aid of LC filter before injecting it into the grid.

5. RESULTS AND DISCUSSION

This study highlights the implementation of Boost integrated Luo converter with PSO-PI controller in the grid-tied EV application, in which the proposed Boost-Luo converter utilities in the process of enhancing output voltage of PV as it owns plenty of beneficial impacts whereas the PSO-PI controller assist in effectively controlling the converter output without any fluctuations. In addition, the converter enhances efficiency and reduces the control complexity. The analytical waveforms are derived for continuous and discontinuous modes of operations. The analysis of dc-voltage gain and boundary conditions are conferred, a 1ϕ VSI is employed to compensate or synchronize the grid voltage through the conversion of DC into AC voltage and output of converter is regulated through the conventional PI controller. The complete research is reviewed in MATLAB Simulink, and the outcomes are fully presented in the following subsection. The converter and PV panel Specifications are listed out in *table 1*.

Table 1: PV panel and Boost-Luo converter specifications

Parameters	Ratings
Operating Voltage	16.8V
No. of series cells	36
Maximum Voltage	1000V
No. of panels	10
Temperature Range	-40 to $+85℃$
Operating Current	5.8A
Converter Ratings	
Diodes	MCD95
L_1, L_2, L_3	0.576mH
C_1, C_2, C_3	300μF
Switching Frequency	$20KH_Z$
Input AC voltage	$170V - 230V$

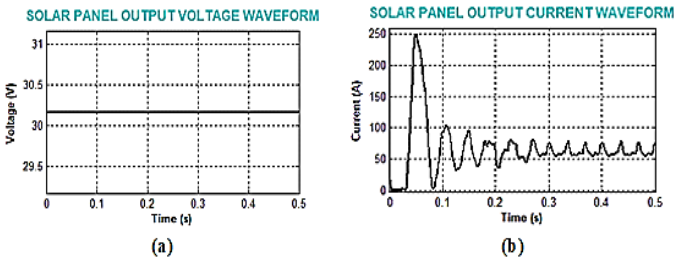

Figure 7: Output voltage and Current Waveforms of PV

The voltage and current outputs of the PV array are remarkably portrayed through the waveforms in *figure 7 (a)* and *(b)*, through which it is highlighted that the PV delivers the voltage of 30.2V as output. Moreover, the raise in the current during the initial stage is maintained after the period of 0.3sec. The reason for increase in current output at initial stage of a PV system is attributed to the sudden exposure of solar panels to sunlight, resulting in a rapid rise in solar irradiance. As a result, the PV panels generate more current in response to the increased sunlight intensity.

FOREX Publication
Open Access | Rapid and quality publishing
International Journal of Electrical and Electronics Research (IJEER)
Research Article | Volume 11, Issue 4 | Pages 1167-1175 | e-ISSN: 2347-470X

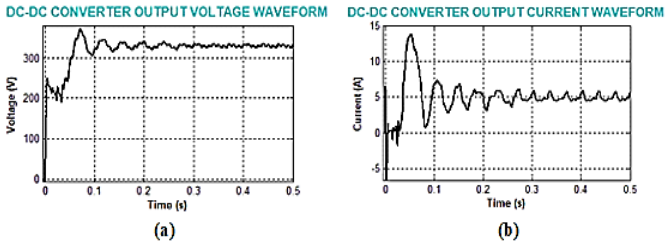

Figure 8: Output voltage and Current Waveforms of Boost-Luo converter

The waveforms indicating voltage and current outputs of proposed converter are evidently illustrated in *figure 8 (a)* and *(b)*, which validates that voltage is highly boosted by the Boost-Luo converter because it delivers the voltage of 3 40V. As depicted in *figure 8 (b)*, the oscillation in the output current is settled after the time of 0.3sec.

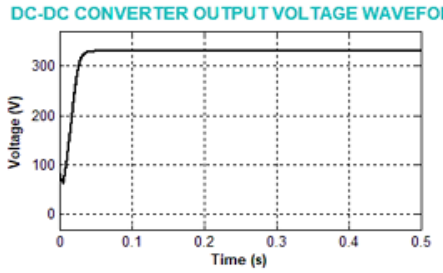

Figure 9: Waveform of converter output voltage using PSO-PI Controller

The fluctuations in converter's output voltage are remarkably eliminated it is constantly retained by the PSO-PI controller as portrayed in *figure 9*, which proves that the converter delivers the constant output without any fluctuations.

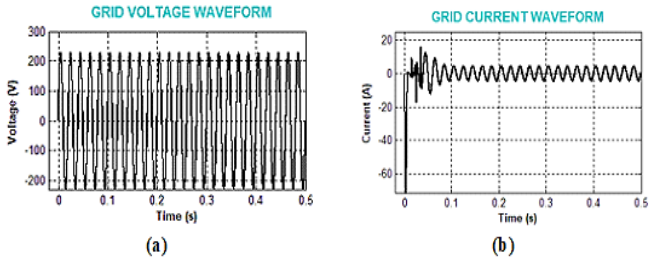

Figure 10: Grid Voltage and Current Waveforms

The waveforms demonstrating voltage and current of grid are significantly shown in *figure 10 (a)* and *(b)*, through which it is noticeable that the grid voltage ranges from -200V to 200V whereas the currents get constantly retained after 0.1sec.

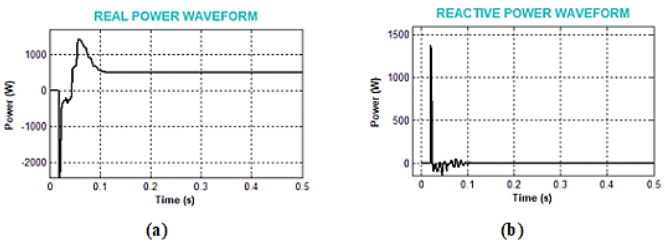

Figure 11: Waveforms of Real and Reactive Powers

The representation of real and complex power waveforms is demonstrated in *figure 11 (a)* and *(b)*, which validates that the real power gets decreased in the initial period but it settles at 500V after the time of 0.1sce. Furthermore, it is witnessed from *figure 11 (b)* that reactive power is settled at zero after 0.1 sec. The initial reduction in real power is due to startup transients. After 0.1 seconds, the system reaches a stable state, and power levels settle down, likely due to the effectiveness of PI control strategy in maintaining the desired power output.

Converter Efficiency:

A converter's efficiency is defined as the ratio of output power to input power. It is typically calculated using the formula:

$$Efficiency = \left(\frac{Output\ Power}{Input\ Power}\right) * 100\% \quad (29)$$

Table 2: Comparison of converters

Converters	Total No. of Components				Efficiency (%)
	Diodes	Switches	inductors	Capacitors	
Boost [32]	1	1	1	1	80
SEPIC [33]	1	1	2	3	88.82
Luo [34]	2	1	1	2	90
Cuk [35]	1	1	2	2	85
Boost-Luo	1	2	3	3	92

Table 3: Comparison of settling time

Control approaches	Settling time (s)
PI [36]	0.4
Fuzzy [37]	0.38
PSO-PI	0.1

The comparison of Boost integrated Luo converter with existing topologies is presented in *table 2* whereas the comparison of the dynamic response of PSO-PI with conventional PI and Fuzzy controllers is listed in *table 3*. PSO-PI's superior dynamic response is due to the ability to adapt and fine-tune control parameters based on real-time optimization, leading to faster and more accurate responses compared to traditional PI or Fuzzy controllers with fixed gains. On comparing, the proposed converter generates an efficiency of 92% while the PSO-PI control aids in generating a settling time of 0.1s.

6. CONCLUSION

The present study exemplifies the significance of Boost integrated Luo converter in the grid linked EV charging station with prior analysis, which signifies that the role of this proposed converter is extremely high in the overall operation of the system because it owns multiple merits like maximum gain ratio and efficiency of 92%. The enhanced converter output is constantly regulated by implementing the PSO assisted PI controller, that involves in eliminating the fluctuations or distortions in the converter output. The integration of battery offers uninterrupted power supply to grid. The converter output is injected to a 1ϕ VSI for compensating the grid voltage whereas the conventional PI controller is employed for

FOREX Publication
Open Access | Rapid and quality publishing
International Journal of Electrical and Electronics Research (IJEER)
Research Article | Volume 11, Issue 4 | Pages 1167-1175 | e-ISSN: 2347-470X

regulating the inverter output as constant. PI controller continuously monitors the error between grid voltage and VSI output voltage, and based on the error, it adjusts the inverter's control signals, enabling precise synchronization with the grid and efficient power transfer. The outcomes have validated that this approach delivers optimal performance with plenty of beneficial impacts. This method provides improved dynamic response with reduced settling time of 0.1s.

REFERENCES

[1] E. Du, N. Zhang, B. Hodge, Q. Wang, C. Kang, B. Kroposki and Q. Xia, "The Role of Concentrating Solar Power Toward High Renewable Energy Penetrated Power Systems", IEEE Transactions on Power Systems, Vol. 33, no. 6, pp. 6630 – 6641, 2018.

[2] H. Klaina, I. P. Guembe, P. Lopez-Iturri, J. J. Astrain, L. Azpilicueta, O. Aghzout, A. V. Alejos and F. Falcone, "Aggregator to Electric Vehicle LoRaWAN Based Communication Analysis in Vehicle-to-Grid Systems in Smart Cities", IEEE Access, vol. 8, pp. 2169-3536, 2020.

[3] Y. Shi, H. D. Tuan, A. V. Savkin, T. Q. Duong and H. V. Poor, "Model Predictive Control for Smart Grids With Multiple Electric-Vehicle Charging Stations", IEEE Transactions on Smart Grid, vol. 10, no. 2, pp. 2127 – 2136, 2019.

[4] E. Taherzadeh, H. Radmanesh and A. Mehrizi-Sani, "A Comprehensive Study of the Parameters Impacting the Fuel Economy of Plug-In Hybrid Electric Vehicles", IEEE Transactions on Intelligent Vehicles, vol. 5, no. 4, pp. 596 – 615, 2020.

[5] S. M. Shariff, M. S. Alam, F. Ahmad, Y. Rafat, M. S. J. Asghar and S. Khan, "System Design and Realization of a Solar-Powered Electric Vehicle Charging Station", IEEE Systems Journal, vol. 14, no. 2, pp. 2748 – 2758, 2020.

[6] D. Yan, H. Yin, T. Li and C. Ma, "A Two-Stage Scheme for Both Power Allocation and EV Charging Coordination in A Grid Tied PV-Battery Charging Station", IEEE Transactions on Industrial Informatics, 2021.

[7] W. Khan, F. Ahmad and M. S Alam, "Fast EV charging station integration with grid ensuring optimal and quality power exchange", Engineering Science and Technology, an International Journal, vol. 22, no. 1, pp. 143-152.

[8] C. Schuss, T. Fabritius, B. Eichberger and T. Rahkonen, "Impacts on the Output Power of Photovoltaics on Top of Electric and Hybrid Electric Vehicles", IEEE Transactions on Instrumentation and Measurement, vol. 69, no. 5, pp. 2449 – 2458, 2020.

[9] A. Verma, B. Singh, A. Chandra and K. Al-Haddad, "An Implementation of Solar PV Array Based Multifunctional EV Charger", IEEE Transactions on Industry Applications, vol. 56, no. 4, pp. 4166 – 4178, 2020.

[10] Sharma, Vanika, Syed Mahfuzul Aziz, Mohammed H. Haque, and Travis Kauschke. "Energy economy of households with photovoltaic system and battery storage under time of use tariff with demand charge." IEEE Access 10 (2022): 33069-33082.

[11] Giglio, Enrico, Gabriele Luzzani, Vito Terranova, Gabriele Trivigno, Alessandro Niccolai, and Francesco Grimaccia. "An efficient artificial intelligence energy management system for urban building integrating photovoltaic and storage." IEEE Access 11 (2023): 18673-18688.

[12] T. Ku and C. Li, "Implementation of Battery Energy Storage System for an Island Microgrid with High PV Penetration", IEEE Transactions on Industry Applications, vol. 57, no. 4, pp. 3416 – 3424, 2021.

[13] Tamilselvi, S., N. Karuppiah, and S. Muthubalaji. "Design of an efficient battery model using evolutionary algorithms." Periodicals of Engineering and Natural Sciences 6.2 (2018): 265-282.

[14] Prasanna Moorthy, V., et al. "A hybrid technique-based energy management in hybrid electric vehicle system." International Journal of Energy Research 46.11 (2022): 15499-15520.

[15] Paide Venkata Narasimha Rao, P.V. Bala Subramanyam, S. MuthuBalaji "Improving the efficiency of Electric vehicle wireless charging system by rectifier load Analysis using ANFIS controller "Journal of Advanced Research in Dynamical & Control Systems, Vol 12., Special issue 3.,PP. 1360-1379 (2020)

[16] A. K. Singh, M. Badoni and Y. N. Tatte, "A Multifunctional Solar PV and Grid Based On-Board Converter for Electric Vehicles", IEEE Transactions on Vehicular Technology, vol. 69, no. 4, pp. 3717 – 3727, 2020.

[17] A. K. Singh, A. K. Mishra, K. K. Gupta, P. Bhatnagar and T. Kim, "An Integrated Converter With Reduced Components for Electric Vehicles Utilizing Solar and Grid Power Sources", IEEE Transactions on Transportation Electrification, vol. 6, no. 2, pp. 439 – 452, 2020.

[18] Gulzar, Muhammad Majid, Ayesha Iqbal, Daud Sibtain, and Muhammad Khalid. "An innovative converterless solar PV control strategy for a grid connected hybrid PV/wind/fuel-cell system coupled with battery energy storage." IEEE Access 11 (2023): 23245-23259.

[19] Roldán-Caballero, Alfredo, Eduardo Hernández-Marquez, Magdalena Marciano-Melchor, José Rafael García-Sánchez, and Gilberto Silva-Ortigoza. "Hierarchical Flatness-Based Control for Velocity Trajectory Tracking of the "DC/DC Boost Converter–DC Motor" System Powered by Renewable Energy." IEEE Access 11 (2023): 32464-32475.

[20] V. A. K. Prabhala, P. Fajri, V. S. P. Gouribhatla, B. P. Baddipadiga and M. Ferdowsi, "A DC–DC Converter With High Voltage Gain and Two Input Boost Stages", IEEE Transactions on Power Electronics, vol. 31, no. 6, pp. 4206 – 4215, 2016.

[21] B. Chandrasekar, C. Nallaperumal, S. Padmanaban, M. S. Bhaskar, J. B. Holm-Nielsen, Z. Leonowicz and S. O. Masebinu, "Non-Isolated High-Gain Triple Port DC–DC Buck-Boost Converter With Positive Output Voltage for Photovoltaic Applications", IEEE Access, vol. 8, pp. 113649 – 113666, 2020.

[22] M. Khodabandeh, E. Afshari and M. Amirabadi, "A Family of Ćuk, Zeta, and SEPIC Based Soft-Switching DC–DC Converters", IEEE Transactions on Power Electronics, vol. 34, no. 10, pp. 113649 – 113666, 2019.

[23] K. Nathan, S. Ghosh, Y. Siwakoti and T. Long, "A New DC–DC Converter for Photovoltaic Systems: Coupled-Inductors Combined Cuk-SEPIC Converter", IEEE Transactions on Energy Conversion, vol. 34, no. 1, pp. 191 – 201, 2019.

[24] S. S Dheeban, N. B. M. Selvan and L. Krishnaveni., "Performance improvement of Photo-Voltaic panels by Super-Lift Luo converter in standalone application", Materials Today: Proceedings, vol. 37, pp. 1163-1171, 2021.

[25] Loganathan and G. Babu., "Design and analysis of high gain Re Boost-Luo converter for high power DC application", Materials Today: Proceedings vol. 33, pp: 13-22, 2020.

[26] Yilmaz, Unal, Ali Kircay and S. Borekci, "PV system fuzzy logic MPPT method and PI control as a charge controller", Renewable and Sustainable Energy Reviews, vol. 81, pp. 994-1001, 2018.

[27] Yanarates, Cagfer, and Zhongfu Zhou. "Design and cascade PI controller-based robust model reference adaptive control of DC-DC boost converter." IEEE Access 10 (2022): 44909-44922.

[28] Asna, Madathodika, H. Shareef, S. N. Khalid, A. Al Dosari, B. Hamad, M. Alhammadi and N. Aldarmaki., "Analysis and design of single phase voltage-frequency converter with optimized PI controller", International Journal of Power Electronics and Drive Systems, vol. 10, no. 1, pp. 522, 2019.

[29] Rajendran, Gowthamraj, Chockalingam Aravind Vaithilingam, Kanendra Naidu, Ahmad Adel Alsakati, Kameswara Satya Prakash Oruganti, and Mohd Faizal Fauzan. "Dynamic voltage stability enhancement in electric vehicle battery charger using particle swarm optimization." IEEE Access 10 (2022): 97767-97779.

[30] T. Eswaran and V. S. Kumar, "Particle swarm optimization (PSO)-based tuning technique for PI controller for management of a distributed static synchronous compensator (DSTATCOM) for improved dynamic response and power quality", Journal of applied research and technology, vol. 15, no. 2, pp. 173-189, 2018.

[31] Bouderres, Nacer, Djallel Kerdoun, Abdelhak Djellad, Sofiane Chiheb, and Azzeddine Dekhane. "Optimization of Fractional Order PI Controller

International Journal of
Electrical and Electronics Research (IJEER)
Research Article | Volume 11, Issue 4 | Pages 1167-1175 | e-ISSN: 2347-470X

by PSO Algorithm Applied to a GridConnected Photovoltaic System." Journal Européen des Systèmes Automatisés 65, no. 4 (2022).

[32] Nejabatkhah, Farzam, Saeed Danyali, Seyed Hossein Hosseini, Mehran Sabahi, and SeyedabdolkhaleghMozaffariNiapour, "Modeling and control of a new three-input DC–DC boost converter for hybrid PV/FC/battery power system," IEEE Transactions on power electronics, vol. 27, no. 5, pp. 2309-2324, 2011.

[33] Javeed, Patan, Lochan Krishna Yadav, P. Venkatesh Kumar, Ranjit Kumar, and Shakti Swaroop, "SEPIC Converter for Low Power LED Applications," In Journal of Physics: Conference Series, vol. 1818, no. 1, p. 012220. IOP Publishing, 2021.

[34] Sivarajeswari, S., and D. Kirubakaran, "Design and development of efficient Luo converters for DC micro grid," The International Journal of Electrical Engineering & Education, pp. 0020720919845152, 2019.

[35] Galea, Francarl, Maurice Apap, Cyril Spiteri Staines, and Joseph Cilia, "Design of a high efficiency wide input range isolated Cuk Dc-Dc converter for grid connected regenerative active loads", 2011.

[36] YILMAZ, Mehmet, Muhammedfatih CORAPSİZ, and Muhammed Reşit ÇORAPSIZ, "Voltage Control of Cuk Converter with PI and Fuzzy Logic Controller in Continuous Current Mode," Balkan Journal of Electrical and Computer Engineering, vol. 8, no. 2, pp. 127-134, 2020.

[37] Rajeswari, R. V., and A. Geetha, "Comparison of Buck-boost and CUK converter control using fuzzy logic controller," Int. J. Innov. Res. Sci. Eng. Technol, vol. 3, no. 3, 2014.